Floquet phonon lasing in multimode optomechanical systems

Laura Mercadé,[1,*] Karl Pelka,[2,*] Roel Burgwal,[3,4] André Xuereb,[2] Alejandro Martinez,[1] and Ewold Verhagen[4,3,†]

[1]*Nanophotonics Technology Center, Universitat Politècnica de Valencia, Spain*
[2]*Department of Physics, University of Malta, Msida MSD 2080, Malta*
[3]*Department of Applied Physics and Institute of Photonic Integration, Eindhoven University of Technology, P.O. Box 513, 5600 MB Eindhoven, The Netherlands*
[4]*Center for Nanophotonics, AMOLF, Science Park 104, 1098 XG Amsterdam, The Netherlands*

(Dated: December 18, 2020)

Dynamical radiation pressure effects in cavity optomechanical systems give rise to self-sustained oscillations or 'phonon lasing' behavior, producing stable oscillators up to GHz frequencies in nanoscale devices. Like in photonic lasers, phonon lasing normally occurs in a single mechanical mode. We show here that phase-locked, multi-mode phonon lasing can be established in a multimode optomechanical system through Floquet dynamics induced by a temporally modulated laser drive. We demonstrate this concept in a suitably engineered silicon photonic nanocavity coupled to multiple GHz-frequency mechanical modes. We find that the long-term frequency stability is significantly improved in the multi-mode lasing state as a result of the phase locking. These results provide a path towards highly stable ultra-compact oscillators, pulsed phonon lasing, coherent waveform synthesis, and emergent many-mode phenomena in oscillator arrays.

is it clear that we can claim it is a result of phase locking?

Introduction.—Recent times have seen an extraordinary progress in exploiting radiation pressure control over optical and mechanical degrees of freedom in cavity optomechanical systems [1]. The combined advantages of high mechanical coherence and quantum-noise-limited optical control allow the generation of pure quantum states of macroscopic mechanical resonators [6, 11] and their use as quantum transducers [36]. The very same advantages lead to highly coherent self-oscillations associated with a parametric instability [2]. Above threshold, a blue-detuned optical drive induces phonon lasing that can be used for timekeeping, signal synthesis, narrowband filters, and to study nonlinear dynamics [3].

Even if multiple mechanical modes are coupled to a cavity, phonon lasing takes place for a single mode whose threshold condition is satisfied first, whilst the other modes get cooled [41] — similar to gain suppression in regular lasers. Simultaneous oscillation in multiple modes was observed in a low-Finesse cavity, but without phase locking. A reliable route to phase-locked phonon lasing opens the door to versatile optomechanical signal synthesis, which is especially valuable at high (GHz) frequencies in chip-scale devices. Moreover, it has broad significance in view of the emergent phenomena in multimode self-oscillating systems, including synchronization [21, 22, 24, 25, 27, 29, 30], stability enhancement [28], dynamical topological phases [20], and analog simulators.

https://www.nature.com/articles/nature03118

addreferences (single-mode), including Eichenfield OM crystals

In this work, we show that the single-mode lasing limitation can be overcome by using a Floquet approach in which the optical drive field is modulated in time. Recently, time-modulated radiation pressure has been used to couple mechanical modes of different frequencies [40] and enable mechanical nonreciprocity [39], synthetic gauge fields [19], and entanglement [12]. Establishing a Floquet theory [37, 38] for phonon lasing, we show that a laser drive modulated at the difference between two mechanical modes' symmetries can lead to phase-locked coherent oscillation of both. We observe the predicted multi-mode lasing in a silicon optomechanical crystal cavity supporting two GHz-frequency mechanical modes. We find that the long-term stability of the output microwave tones is significantly improved, showing that the mechanisms can be exploited towards highly stable, ultra-compact oscillators for microwave photonics.

or mode competition?

https://journals.aps.org/pr/abstract/10.1103/PhysRev.134.A1429

https://journals.aps.org/prl/pdf/10.1103/PhysRevLett.101.133903

https://advances.sciencemag.org/content/2/6/e1600236.full

Theoretical model.—We consider the collective dynamics of a system consisting of N mechanical modes (labeled by j) coupled to one optical mode, described by the Hamiltonian

$$\hat{H}_S/\hbar = \omega_{op}\hat{a}^\dagger\hat{a} + \sum_{j=1}^{N}\left[\Omega_j\hat{b}_j^\dagger\hat{b}_j - g_j\hat{a}^\dagger\hat{a}(\hat{b}_j + \hat{b}_j^\dagger)\right], \quad (1)$$

with $\hat{a}$ ($\hat{b}_j$) the optical (mechanical) annihilation operator, ω_{op} (Ω_j) the resonance frequency, and g_j the vacuum optomechanical coupling rates. The laser driving the cavity is modelled by adding $i\hbar[\mathcal{E}_{drive}(t)\hat{a}^\dagger - \mathcal{E}^*_{drive}(t)\hat{a}]$ to the Hamiltonian, where we assume $\mathcal{E}_{drive}(t) = \mathcal{E}_0 e^{i\omega_L t}\mathcal{T}(t)$ and $\mathcal{T}(t)$ describes amplitude modulation. Appending bath degrees of freedom and tracing them out [1] yields quantum Langevin equations. These can be separated into mean field and fluctuation components of the mechanical and optical degrees of freedom ($\hat{a}(t)e^{i\omega_L t + i\phi_0} = \alpha(t) + \hat{\mathfrak{a}}(t)$ and $\hat{b}_j(t) = \beta_j(t) + \hat{\mathfrak{b}}_j(t)$), with mean fields obeying

implements intensity modulation

$$\dot{\alpha} = \left\{-i\left[\Delta - \sum_{j=1}^{N} g_j \mathrm{R}(\beta_j)\right] - \frac{\kappa}{2}\right\}\alpha + \mathcal{E}_0\mathcal{T}e^{-i\phi_0},$$
$$\dot{\beta}_j = -\left(i\Omega_j + \frac{\Gamma_j}{2}\right)\beta_j + ig_j|\alpha|^2, \quad (2)$$

and linearized dynamics for the fluctuations

$$\dot{\hat{\mathfrak{a}}} = -\left(i\Delta + \frac{\kappa}{2}\right)\hat{\mathfrak{a}} + i\sum_{j=1}^{N} g_j[\alpha\Re(\hat{\mathfrak{b}}_j) + \hat{\mathfrak{a}}\mathrm{R}(\beta_j)] + \sqrt{\kappa}\hat{\mathfrak{a}}_{in},$$
$$\dot{\hat{\mathfrak{b}}}_j = -\left(i\Omega_j + \frac{\Gamma_j}{2}\right)\hat{\mathfrak{b}}_j + ig_j(\alpha^*\hat{\mathfrak{a}} + \alpha\hat{\mathfrak{a}}^\dagger) + \sqrt{\Gamma_j}\hat{\mathfrak{b}}_{j,in}. \quad (3)$$

* These authors contributed equally to this work
† verhagen@amolf.nl

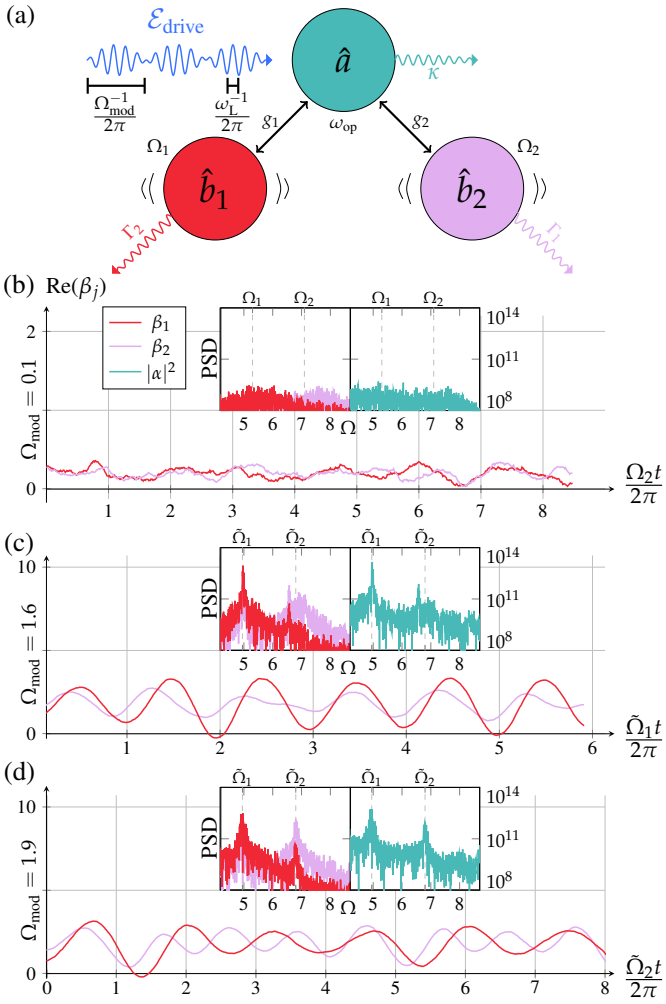

FIG. 1. (Color online) Multi-mode phonon lasing in a optomechanical cavity. (a) Schematics of the system under consideration: two mechanical modes at distinct frequencies are coupled to an optical mode via photon radiation pressure and driven by an intensity modulated pump tone. (b) For a modulation frequency which is much smaller than the difference frequency both mechanical modes result in a thermal state. (c) With the modulation frequency approaching the difference frequency one mode starts self-sustained oscillations (SSO) and the other mode is driven as in the usual mode competition setting. (d) For a modulation frequency which is approximately the difference frequency both mechanical modes start to coherently oscillate at distinct frequencies, i.e. multi-mode oscillations (MMO) occur. The insets show the power spectral densities of the mechanical (left) and optical (right) modes in the respective configurations. The numerical method and parameters for the simulations are discussed in the main text.

Here, the optical field is considered in a rotating frame with respect to the central laser frequency $\omega_{\rm L}$ such that $\Delta = \omega_{\rm op} - \omega_{\rm L}$ denotes the detuning of the central laser frequency from the optical resonance, $\Re(\hat{o}) = \hat{o} + \hat{o}^\dagger$, and $\mathrm{R}(z) = z + z^*$. For a periodic modulation $\mathcal{T}(t) = \sum_k \mathcal{T}_k e^{-ik\Omega_{\rm mod}t}$, the equation for the mean optical field α inherits the periodicity. Hence, we choose a Floquet ansatz and express α as a truncated Fourier series $\alpha(t) = \sum_n \alpha_n e^{-in\Omega_{\rm mod}t}$ with $n \in \{-D, ..., D\}$ and find that Eq. (2) reduces to the dynamical system

$$\dot{\alpha}_m = \mathcal{E}_0 \mathcal{T}_m - \tilde{\chi}_{{\rm cav},m}^{-1}\alpha_m + \sum_{(p,q)} \chi_{{\rm cub},q}^{-1}\alpha_p\alpha_{p-q}^*\alpha_{m-q}, \quad (4)$$

where $p \in \{-D, ..., D\}$, $q \in \{-D+p, ..., D+p\}$, and the solutions of the mechanical mean fields $\beta_j(t)$ follow from their solutions in Fourier space. Here, we defined $\tilde{\chi}_{{\rm cav},m}^{-1} = i(\Delta - m\Omega_{\rm mod}) + \frac{\kappa}{2}$, $\tilde{\chi}_{{\rm me},mj}^{-1} = i(\Omega_j - m\Omega_{\rm mod}) + \frac{\Gamma_j}{2}$, and $\chi_{{\rm cub},q}^{-1} = \sum_j \chi_{{\rm OM},j}^{-1}(q\Omega_{\rm mod})$, with $\chi_{{\rm OM},j}^{-1}(\omega)/g_j^2 = [i(\omega - \Omega_j) - \frac{\Gamma_j}{2}]^{-1} - [i(\omega + \Omega_j) - \frac{\Gamma_j}{2}]^{-1}$. Finding the steady state ($\dot{\alpha}_m = 0$) requires the solution of $2D+2$ coupled real cubic equations which has to be done numerically beyond $D = 0$. Employing the resulting steady state $\bar{\alpha}_m$ turns the dynamics of fluctuation components $\hat{\mathfrak{a}}$ and $\hat{\mathfrak{b}}$ into a periodic system which can be treated with Floquet techniques [37]:

$$\begin{aligned}
\dot{\hat{\mathfrak{a}}}^{(m)} =& -\tilde{\chi}_{{\rm cav},m}^{-1}\hat{\mathfrak{a}}^{(m)} - \sum_{(p,q)}\sum_{j=1}^{N}\chi_{{\rm OM},jq}^{-1}\bar{\alpha}_p\bar{\alpha}_{p-q}^*\hat{\mathfrak{a}}^{(m-q)} \\
&+ \sum_{n=-D}^{D}\sum_{j=1}^{N} ig_j\bar{\alpha}_{-n}\Re(\hat{\mathfrak{b}}_j^{(m-n)}) + \sqrt{\kappa}\hat{\mathfrak{a}}_{\rm in}^{(m)}, \\
\dot{\hat{\mathfrak{b}}}_j^{(m)} =& -\tilde{\chi}_{{\rm me},mj}^{-1}\hat{\mathfrak{b}}_j^{(m)} + ig_j\sum_{n=-D}^{D}\left[\bar{\alpha}_{-n}^*\hat{\mathfrak{a}}^{(m-n)} + \bar{\alpha}_n\hat{\mathfrak{a}}^{\dagger(m-n)}\right] \\
&+ \sqrt{\Gamma_j}\hat{\mathfrak{b}}_{j,{\rm in}}^{(m)}. \qquad (5)
\end{aligned}$$

Using the input–output relations for the relevant contributions of the optical field $\hat{\mathfrak{a}}_{\rm out}(\omega) = \hat{\mathfrak{a}}_{\rm in}^{(0)}(\omega) - \sqrt{\kappa}\hat{\mathfrak{a}}^{(0)}(\omega)$ with input noise obeying $\langle\hat{\mathfrak{u}}_{\rm in}^{(m)}(\omega)\hat{\mathfrak{w}}_{\rm in}^{\dagger(n)}(\omega')\rangle = \delta(\omega - \omega')\delta_{\mathfrak{u}\mathfrak{w}}\delta_{mn}(\mathfrak{n}_{\rm th}^{\mathfrak{u}} + 1)$ leads to the stationary power spectral density of the output field consisting of a noise floor $\tilde{S}$ and multiple Lorentzian peaks proportional to $\mathfrak{n}_{\rm th}^{\mathfrak{b}_j} \equiv \bar{n}_j$

$$S(\omega) = \tilde{S} + \sum_{p,j}\frac{\kappa g_j^2|\bar{\alpha}_p|^2\Gamma_j\bar{n}_j}{\left[(\omega - \tilde{\Delta})^2 + \frac{\tilde{\kappa}^2}{4}\right]\left[(\omega - \Omega_{jp})^2 + \frac{\Gamma_j^2}{4}\right]} \quad (6)$$

located at $\Omega_{jp} = \Omega_j + p\Omega_{\rm mod}$ and filtered by the cavity density of states. This is of Lorentzian form, with frequency-independent effective detuning $\bar{\Delta} = \Delta - \sum_{j,p}\frac{2g_j|\bar{\alpha}_p|^2}{\Omega_j}$, due to the static radiation pressure, modified to $\tilde{\Delta}(\omega) = \bar{\Delta} + \sum_{j,p}|\bar{\alpha}_p|^2\mathrm{Im}(\chi_{{\rm OM},j}^{-1}(\omega + p\Omega_{\rm mod}))$ and the effective linewidth $\frac{\tilde{\kappa}}{2}(\omega) = \frac{\kappa}{2} + \sum_{j,p}|\bar{\alpha}_p|^2\mathrm{Re}(\chi_{{\rm OM},j}^{-1}(\omega + p\Omega_{\rm mod}))$.

Stability analysis.—In order to evaluate the stability of the mechanical motion, we can eliminate the optical field fluctuation operator $\hat{\mathfrak{a}}^{(0)}$ and analyze its effect on the Floquet modes

of the mechanical oscillators

$$\hat{\mathfrak{b}}_j^{(m)}[\tilde{\chi}_{\mathrm{me},mj}^{-1} - i\omega] = \sqrt{\Gamma_j}\hat{\mathfrak{b}}_{j,\mathrm{in}}^{(m)} - \sum_{l,p}\sigma_{jlp}^{(m)}(\omega)\Re(\hat{\mathfrak{b}}_l^{(p)}) + i\sqrt{\kappa}g_j\left[\frac{\bar{\alpha}_{-m}^*\hat{\mathfrak{a}}_{\mathrm{in}}^{(0)}}{i(\bar{\Delta}-\omega)+\frac{\kappa}{2}} + \frac{\bar{\alpha}_m\hat{\mathfrak{a}}_{\mathrm{in}}^{(0)\dagger}}{-i(\bar{\Delta}+\omega)+\frac{\kappa}{2}}\right], \quad (7)$$

coupling the mechanical Floquet modes via the contributions

$$\sigma_{jlp}^{(m)}(\omega) = \frac{g_j g_l \bar{\alpha}_{-m}^* \bar{\alpha}_p}{i(\bar{\Delta}-\omega)+\frac{\kappa}{2}} - \frac{g_j g_l \bar{\alpha}_m \bar{\alpha}_p^*}{-i(\bar{\Delta}+\omega)+\frac{\kappa}{2}}. \quad (8)$$

Without periodic drive ($m \equiv p \equiv 0$), the stationary mechanical spectra are $S_{\hat{\mathfrak{b}}_j}(\omega) = \tilde{S}_{\hat{\mathfrak{b}}_j} + \Gamma_j\bar{n}_j[(\Omega_j'-\omega)^2 + \Gamma_j'^2/4]^{-1}$ with modified mechanical frequencies and decay rates [48, 49]

$$\Omega_j'(\omega) = \Omega_j\sqrt{1 - \frac{\bar{\Delta}g_j^2|\bar{\alpha}_0|^2[\frac{\kappa^2}{4} - \omega^2 + \bar{\Delta}^2]}{\Omega_j[\frac{\kappa^2}{4} + (\omega-\bar{\Delta})^2][\frac{\kappa^2}{4} + (\omega+\bar{\Delta})^2]}},$$
$$\Gamma_j'(\omega) = \Gamma_j + \frac{4\kappa g_j^2|\bar{\alpha}_0|^2\bar{\Delta}\omega}{[\frac{\kappa^2}{4} + (\omega-\bar{\Delta})^2][\frac{\kappa^2}{4} + (\omega+\bar{\Delta})^2]}. \quad (9)$$

These expressions can be used to assess the stability of the mechanical oscillators: The mechanical decay rate Γ_j' is composed of decay of phonons into the bath Γ_j which can be counteracted by the stimulated emission process for blue-detuned driving ($\bar{\Delta} < 0$). In the stimulated emission process for the respective oscillator $\omega = \Omega_j$, a cavity photon with excess energy and a phonon are converted into a resonant photon and two coherent phonons of this mode and its rate overcoming the decay rate Γ_j indicates the onset of self-sustained oscillation at frequency Ω_j. In the presence of the periodic drive, there are additional contributions that modify the mechanical decay rates

$$\Gamma_j''(\Omega_j) = \Gamma_j' - \sum_{l,p}\mathrm{Re}\left[\frac{(1-\delta_{jl}\delta_{p0})\sigma_{jlp}^{(0)}\sigma_{jl0}^{(p)}}{i(\Omega_l - \Omega_{jp}) + \frac{\Gamma_l}{2} + \sigma_{jlp}^{(p)}}\right], \quad (10)$$

which can become prominent if the modulation frequency is tuned to the difference of distinct mechanical frequencies $\Omega_{\mathrm{mod}} = \pm(\Omega_j - \Omega_l)$ with and $j \neq l$ for low modulation depths ($|\bar{\alpha}_{\pm 1}|^2 \ll |\bar{\alpha}_0|^2$). These additional contributions can be interpreted as the stimulated emission of a cavity photon and a phonon creating a coherent phonon in a different mode. This process can act as a seed of phase-locking between the two mechanical modes. Additionally, Eq. (9) include the optical spring effect suggesting that the central frequencies of each oscillator Ω_j' vary jointly based on uncertainties in the mean intensity $\delta|\bar{\alpha}_0|^2$ and the effective detuning $\delta\bar{\Delta}$.

To verify the existence of the multi-mode phonon lasing state, we conduct a numerical simulation of the Itô stochastic differential equation corresponding to Eq. (2) as depicted in Fig. 1. The periodic drive is included by using the transfer function of a Mach-Zehnder intensity modulator (see SI). We employ the Euler–Maruyama scheme [50] by adding Gaussian noise terms $\xi_l(t)$ with zero mean $\langle\xi_k(t)\rangle = 0$ and time correlation $\langle\xi_k(t)\xi_l(t')\rangle = \delta_{kl}\lambda_l\delta(t-t')$ for all $2(N+1)$ components. We choose an instructive set of parameters for two mechanical modes ($N = 2$), namely $\Omega_1 = 5.3$, $\Gamma_1/\Omega_1 = 0.16$, $g_1 = 0.80$, $\Omega_2 = 7.1$, $\Gamma_2/\Omega_2 = 0.10$, $g_1 = 1.1$ as well as the optical cavity $\Delta = 6.1$, and $\kappa = 3$ which places the example in the resolved sideband regime. We keep all parameters within two orders of magnitude because stiff stochastic differential equations, having parameters varying over several orders of magnitude, cannot easily be simulated numerically. To initialize the system, we evolve it without drive ($\mathcal{E}_0 = 0$) and let it thermalize under cavity shot noise [51], i.e. $\langle\xi_k(t)\xi_l(t')\rangle = \delta_{\alpha l}\delta_{lk}\delta(t-t')$. To probe the stability of the attractor, we then drive this system with $\mathcal{E}_0 = 8.9$ and phonon noise $\langle\xi_k(t)\xi_l(t')\rangle = 0.01\delta_{\beta l}\delta_{lk}\delta(t-t')$. Using the modulation depth of $d = 0.08$ while varying modulation frequencies Ω_{mod} reveals the effect of the intensity modulation. Figure 1(b) shows that for off-resonant intensity modulation the mechanical modes evolve in a thermal state. At intermediate modulation frequency, one of the two oscillators transitions into self-sustained oscillations while the other is driven at this same frequency, as depicted in Fig. 1(c). Tuning the modulation frequency to approximately the difference of the mechanical frequencies shows that both mechanical degrees now undergo coherent oscillation at distinct frequencies as can be seen in Fig. 1(d). We coin this operation multi-mode oscillation (MMO) since the respective peaks in the mechanical spectra are described by Lorentzians with a decreased linewidth and not by the sum of the thermal Lorentzian and a sideband.

Experimental multimode phonon lasing.—In our experiments, we used the 1D silicon optomechanical crystal cavity depicted in Fig. 2(a). This cavity gives rise phonon lasing at frequencies around 4 GHz under blue-detuned laser driving [53]. Interestingly, this kind of cavity supports a set of mechanical modes with frequencies within a phononic bandgap that can physically be identified with oscillations of the lateral corrugations [52]. Therefore, it is a highly interesting platform to observe physics related to multimode phononics. The fabricated cavity supports a high-quality optical mode, as shown in Fig. 2(b) and, at least, two mechanical modes, P1 and P2, as depicted in Fig. 2(c). Notice that the cavity dimensions were retrieved from the real profile obtained from the SEM image and then simulated numerically to get the optical and mechanical field profiles. In Fig. 2(d) the thermally-transduced power spectral density of both mechanical modes is shown. All these measurements were performed at room temperature and atmospheric pressure by coupling the light into and out of the cavity with a dimple fiber taper. Notably, the coupling rate and mechanical leakage of both mechanical modes are quite similar, which also leads to a similar cooperativity, defined as $C_0 = (4g_0^2)/(\Gamma_m\kappa)$, $C_{0,1} = (5.6 \pm 0.4) \times 10^{-5}$ for mode P1 and $C_{0,2} = (3.7 \pm 0.3) \times 10^{-5}$ for mode P2. This means that both modes could be individually driven to a phonon lasing state, since their features are similar to the mechanical mode employed in [53].

In our cavity, the two mechanical modes can separately reach the self-sustained oscillation regime under blue-detuned

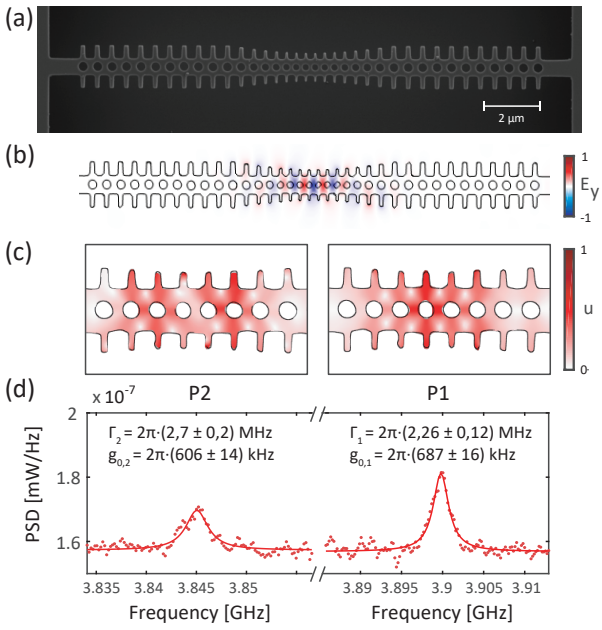

FIG. 2. (a) Scanning electron microscope (SEM) image of the fabricated optomechanical cavity used in this work; (b) Simulated electric field pattern of the localized optical mode in the fabricated cavity. The optical mode was measured to have a resonant wavelength λ_r=(1527.4±0.2) nm with a loaded optical quality factor of Q_o=(1.32±0.1)×10^4 and an overall decay rate of $\kappa/2\pi$=(14.88±0.08) GHz. (c) Calculated mechanical displacement profiles of the two involved mechanical modes P1 and P2. (d) Measured power spectral density of the thermally-transduced mechanical modes P1 and P2. The measurements allows us to describe the two mechanical modes as follows: resonant frequencies $\Omega_1/2\pi$=3.899 GHz and $\Omega_2/2\pi$=3.845 GHz with mechanical linewidths $\Gamma_1/2\pi$=(2.26±0.12) MHz and $\Gamma_2/2\pi$=(2.7±0.2) MHz and measured optomechanical coupling rates $g_{0,1}/2\pi$=(687±16) kHz and $g_{0,1}/2\pi$=(606±14) kHz.

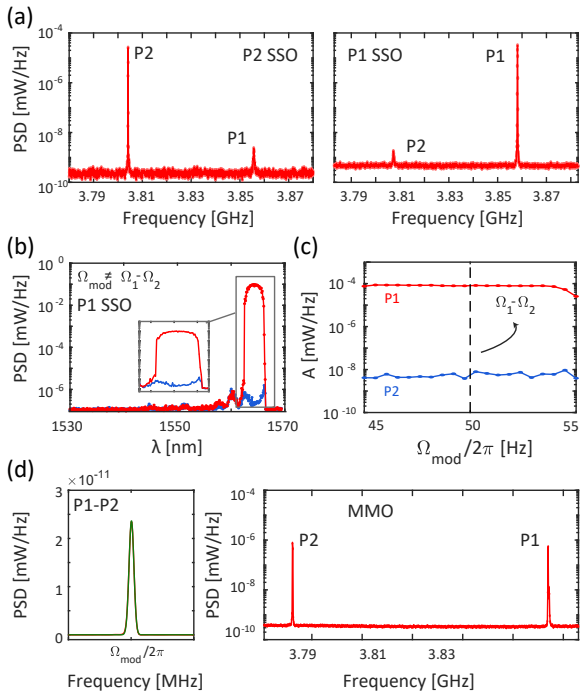

FIG. 3. From single mode to multimode phonon lasing. (a) Self oscillation spectra of P2 (left) and P1 (right), without external modulation. (b) P1 SSO exitation through a wavelength scan with a blue detuned laser respecto to the optical resonance $\Omega_{\rm mod} \neq \Omega_1 - \Omega_2$. (c) Modulation frequency scan around the difference frequency when P1 is self oscillating. (d) MMO excitation through a wavelength scan when $\Omega_{\rm mod} = \Omega_1 - \Omega_2$. (e) Multimode lasing under an input modulation of $\Omega_{\rm mod} = \Omega_1 - \Omega_2$. (First panel) Difference tone resulting from the interaction between the two lasing mechanical modes. (Second panel) View of the two simultaneously lasing mechanical modes.

driving, in accordance with [41], as shown in Fig. 3(a,b). The choice of the lasing state cannot be determined *a priori*, and depends strongly on the experimental conditions as the coupling efficienty between the cavity and the dimple taper cavity coupled at the close vicinity of the cavity. An example of the driving scheme of a single self oscillating mechanical mode is presented in Fig. 3(c), where a sweep in the laser wavelength is performed at an laser input power of $P_{in} = 3.16$ mW at a modulation driving tone $\Omega_{\rm mod} \neq \Omega_1 - \Omega_2$. Here, we can see that once one of the mechanical modes has reach the lasing state, the other mechanical mode P2 is damped **??**. Following the theoretical results, we introduce a modulation of the driving tone by a periodic signal of frequency $\Omega_{\rm mod} = \Omega_1 - \Omega_2$. However, if a sweep in the modulation frequency is performed once one the mechanical modes is already in the SSO regime, the MMO will not be activated, as can be appreciated in Fig. 3(c). Here, we show the amplitude of the modes depicted in Fig. 3(b) once P1 was in the SSO regime and $\Omega_{\rm mod}$ is change across the difference frequency P1-P2. To reach the MMO regime the experiment was performed as follows: First, the difference frequency between the two involved mechanical modes was characterized at different laser wavelengths. Next, this difference frequency was set as the modulation frequency of the laser driving the cavity, and it was kept constant in the rest of the experiment. Finally, a sweep of the laser wavelength on the blue-detuned side of the resonance was performed, reaching in this way the multimode laser regime as depicted in the second panel of Fig. 3(d). We were also able to see both the difference $\Omega_1 - \Omega_2$, shown in the first panel of Fig. 3(d), if we send the detected signal through a microwave mixer, which confirms the mode-locking between P1 and P2. Here, it has to be noted that this is not the modulation frequency tone given by the intensity modulator used in our experiment, as it is filtered in our experimental scheme for the detection configuration. This signal corresponds to the difference P1-P2 generated by the interference betweem P1 and P2 in the mixer set between the photodetector and the cavity. Further details regarding the experimental setup can be found in the Supplementary Material. This measurements was performed at a frequency span of 20 MHz and a resolution bandwidth of 1 Hz but it was limited by the Gaussian filter of the real spectrum analyzer used in our experiments.

Phase noise and stability analysis.— In order to character-

ize the linewidth and stability of the oscillators, we analyzed first the phase noise of the mechanical oscillators in both the single and multimode phonon lasing states. Fig. 4(a,b) shows the phase noise $L(f)$ when P2 is lasing and P1 is thermally activated (as in Fig. 3(a)) because there is no external modulation. In both cases (SSO and MMO), we observe the different noise contributions that can be expected in optomechanical oscillators, in particular, the white phase $(1/f^0)$, white frequency, also called random phase walk, $(1/f^2)$ and flicker frequency $(1/f^3)$ noise types [53], being in good agreement with the Leeson's model [56]. Phase noise values around -100 dBc/Hz at 100 kHz were observed, in agreement with [53], which means that our device could be used as an optomechanical microwave oscillator even when operated at room temperature. This value is highly competitive with other optomechanical microwave oscilators as MEMS oscillators [61], Si 2D photonic crystal cavities [57] or SiN ring resonators [60]. From the fit of the random phase walk $(1/f^2)$ at Fig. 4(a,b) a Lorenztian linewidth of $\Gamma_{eff,P2}/2\pi \simeq 31$ Hz is extracted fot P2 in the SSO and $\Gamma_{eff,P1}/2\pi \simeq 37$ Hz and $\Gamma_{eff,P1}/2\pi \simeq 36$ Hz for P1 and P2 in the MMO, respectively. It has to be noted that these values are slighly lower than in the case of other reported optomechanical GHz oscillators [59].

The time evolution of the recorded spectra for both single mode and multimode lasing are presented in Fig. 4(c,d), where the top panel corresponds to P1 and the bottom to P2. A small jitter of the lasing frequency can be appreciated even with the naked eye. We attribute the time jitter to the coexistence of multiple competing physical phenomena (thermo-optic nonlinearity, free-carrier refraction and absorption, optomechanical interaction) as well as slow variations of the tapered fiber. However, when the external modulation is active, the two mechanical modes are phase-locked, which results in an improvement of the long-term stability of the oscillation frequencies in time (4(d)), remarkably improving the performance of a single oscillator.

In order to further characterize the frequency stability of the mechanical oscillators, we use the Allan deviation $\sigma(\tau)$ [54]. The resulting calculated Allan deviation for the lasing modes is presented in Fig. 4(f) for both the single and multimode lasing states. Here, two different calculations of the Allan deviation have been considered. For small averaging times, the Allan deviation was considered to be the one obtained from the phase noise measurements in Fig. 4(a,b), taking into account the contributions of the random walk phase and the flicker frequency noise. For large τ, the parameter was estimated from the measurement of the evolution of the oscillation frequency as a function of time as measured by a real-time electrical spectrum analyzer. Further details regarding these calculations are exposed in the Supplementary Material. Here, we can see that for low τ, the SSO and the MMO performs in the same way. Differences at even lower τ values may be appreciated if we consider the white phase noise, but may be attributed to the lasing peak amplitude. However, the MMO performs better in the long-term as a result of the locking between the mechanical modes. This improvement in the frequency drift contribution of the Allan deviation may be related with the driving force amplitude because the MMO regime occurs at less power in the cavity compared to the SSO, as it was observed in 3. This reduction of the intensity should yield, through a propagation uncertainty analysis (See Supplementary Material for more details (TBC- Karl's already distributed estimation)), a reduction of the frequency deviation and thus providing a stabilization in the frequency [62].

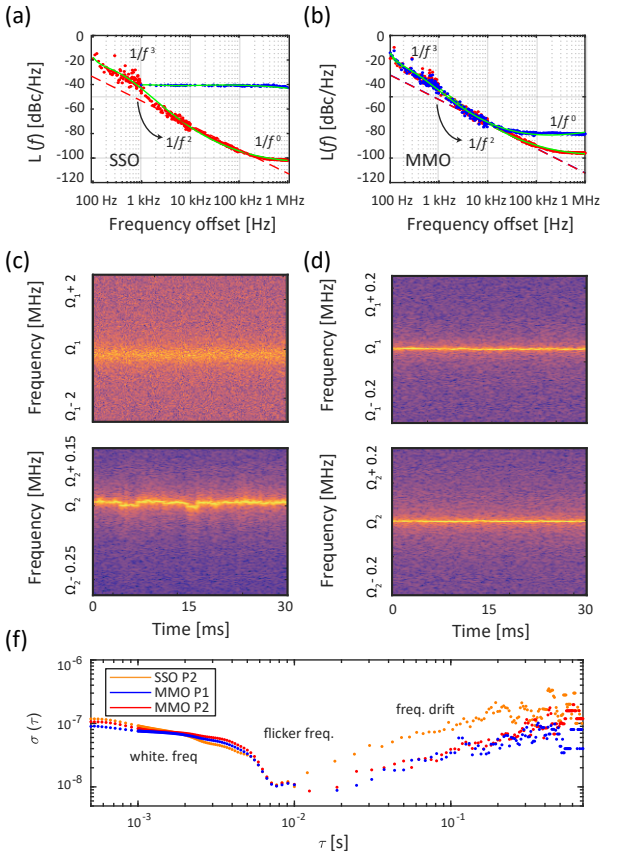

FIG. 4. Phase noise and stability behaviour. Phase noise of P1 (blue) and P2 (red) in the single phonon lasing regime (SSO) when P2 is lasing (a) and in the multimode lasing regime (b). Frequency evolution in the SSO for P1 (top panel) and P2 (bottom panel) under SSO (c) and MMO lasing (d). (f) Allan deviation for P2 (SSO) and P1 and P2 (MMO).

Conclusion.—Our investigation shows that non-linear dynamics of Floquet modes can be used to enable multi-mode phonon lasing in optomecanical systems. The analytical argument based on higher order corrections of the self-energy being resonant for intensity modulation at the difference of the mechanical frequencies is underpinned by numerical simulations as well as an experimental demonstration. We show that multimode phonon lasing becomes feasible when using an external signal that modulates the driving laser. Moreover, we also show the improvement in the long-term stability in the multimode lasing case. The multimode cavity used in our experiments can pave the way towards to integration of multiple coexisting GHz mechanical modes whose frequencies can be slightly tuned by engineering the height and width of the lateral corrugations. Moreover, this family of mechanical modes can be located within a complete phononic bandgap [53],

which should lead to very large mechanical quality factors when working in cryogenic environments.

This work is supported by the European Union's Horizon 2020 research and innovation programme under Grant Agreements Nos. 732894 (FET Proactive HOT), 713450 (FET-Open PHENOMEN), and 945915 (SIOMO). A.M. acknowledges funding from Generalitat Valenciana under grants PROMETEO/2019/123, BEST/2020/178, IDIFEDER/2018/033). L.M. acknowledges great help and support from the Photonic Forces Group in Amolf during the measurement campaign.

[1] M. Aspelmeyer, T. J. Kippenberg, and F. Marquardt, Rev. Mod. Phys **86**, 1391 (2014).
[2] T. J. Kippenberg, H. Rokhsari, T. Carmon, A. Scherer, and K. J. Vahala, Phys. Rev. Lett. **95**, 033901 (2005).
[3] F. Marquardt, J. G. E. Harris, and S. M. Girvin, Phys. Rev. Lett. **96**, 103901 (2006).
[4] S. Gröblacher, K. Hammerer, M. R. Vanner, and M. Aspelmeyer, Nature (London) **460**, 724 (2009).
[5] J. D. Thompson, B. M. Zwickl, F. Marquardt, S. M. Girvin, and J. G. E. Harris, Nature (London) **452**, 72 (2008).
[6] J. D. Teufel, T. Donner, D. Li, J. W. Harlow, M. S. Allman, K. Cicak, A. J. Sirois, J. D. Whittaker, K. W. Lehnert, and R. W. Simmonds, Nature (London) **475**, 359 (2011).
[7] J. Millen, T. Deesuwan, P. Barkere, and J. Anders, Nat. Nanotechnol. **9**, 425 (2014).
[8] U. Delić, M. Reisenbauer, D. Grass, N. Kiesel, V. Vuletić, and M. Aspelmeyer, Phys. Rev. Lett. **122**, 123602 (2019).
[9] E. Gil-Santos, C. Baker, A. Lemaître, S. Ducci, C. Gomez, G. Leo, and I. Favero, Nat. Commun. **8**, 14267 (2017).
[10] W.-M. Zhang, K.-M. Hu, Z.-K. Peng, and G. Meng, Sensors **15**, 26478 (2015).
[11] J. Chan, T. P. M. Alegre, A. H. Safavi-Naeini, J. T. Hill, A. Krause, S. Gröblacher, M. Aspelmeyer, and O. Painter, Nature (London) **475**, 359 (2011).
[12] C. F. Ockeloen-Korppi, E. Damskägg, J. M. Pirkkalainen, M. Asjad, A. A. Clerk, F. Massel, M. J. Wooley, and M. A. Sillanpää, Nature (London) **556**, 478 (2018).
[13] R. Riedinger, A. Wallucks, I. Marinković, C. Löschnauer, M. Aspelmeyer, S. Hong, and S. Gröblacher, Nature (London) **556**, 473 (2018).
[14] A. Xuereb, C. Genes, and A. Dantan, Phys. Rev. Lett. **109**, 223601 (2012).
[15] P. Piergentili, L. Catalani, M. Bawaj, S. Zippilli, N. Malossi, R. Natali, D. Vitali, and G. Di Giuseppe, New J. Phys. **20**, 083024 (2018).
[16] M. Schmidt, S. Kessler, V. Peano, O. Painter, and F. Marquardt, Optica **2**, 635 (2015).
[17] V. Peano, C. Brendel, M. Schmidt, and F. Marquardt, Phys. Rev. X **5**, 031011 (2015).
[18] H. Ren, T. Shah, H. Pfeifer, C. Brendel, V. Peano, F. Marquardt, and O. Painter, arXiv:2009.06174 **v.xyz**, p.xyz (2020).
[19] J. P. Mathew, J. del Pino, and E. Verhagen, Nat. Nanotechnol. **15**, 198 (2020).
[20] S. Walter, and F. Marquardt, New J. Phys. **18**, 113029 (2016).
[21] G. Heinrich, M. Ludwig, J. Qian, B. Kubala, and F. Marquardt, Phys. Rev. Lett. **107**, 043603 (2011).
[22] R. Lauter, C. Brendel, S. J. M. Habraken, and F. Marquardt, Phys. Rev. E **92**, 012902 (2015).
[23] R. Lauter, A. Mitra, and F. Marquardt, Phys. Rev. E **96**, 012220 (2017).
[24] C. A. Holmes, C. P. Meaney, and G. J. Milburn, Phys. Rev. E **85**, 066203 (2012).
[25] N. Lörch, S. E. Nigg, A. Nunnenkamp, R. P. Tiwari, and C. Bruder, Phys. Rev. Lett **118**, 243602 (2017).
[26] E. Amitai, N. Lörch, A. Nunnenkamp, S. Walter, and C. Bruder, Phys. Rev. A **95**, 053858 (2017).
[27] M. Zhang, G.S. Wiederhecker, S. Manipatruni, A. Barnard, P. McEuen, and M. Lipson, Phys. Rev. Lett. **109**, 233906 (2012).
[28] M. Zhang, S. Shah, J. Cardenas, and M. Lipson, Phys. Rev. Lett. **115**, 163902 (2015).
[29] M. F. Colombano, G. Arregui, N. E. Capuj, A. Pitanti, J. Maire, A. Griol, B. Garrido, A. Martinez, C. M. Sotomayor-Torres, and D. Navarros-Urrios, Phys. Rev. Lett. **123**, 017402 (2019).
[30] K. Pelka, V. Peano, and A. Xuereb, Phys. Rev. Research **123**, 017402 (2019).
[31] G. Madiot, F. Correia, S. Barbay, and R. Braive, arXiv:2005.08896 **v.xyz**, p.xyz (2020).
[32] N. R. Bernier, L. D. Tóth, A. Koottandavida, M. D. Ioannu, D. Malz, A. Nunnenkamp, A. K. Feofanov, and T. J. Kippenberg, Nat. Commun. **8**, 604 (2017).
[33] D. Malz, L. D. Tóth, N. R. Bernier, A. K. Feofanov, T. J. Kippenberg, and A. Nunnenkamp, Phys. Rev. Lett. **120**, 023601 (2018).
[34] S. Barzanjeh, M. Wulf, M. Peruzzo, M. Kalaee, P. B. Dieterle, O. Painter, and J. M. Fink, Nat. Commun. **8**, 953 (2017).
[35] L. Mercier de Lépinay, E. Damskägg, C. F. Ockeloen-Korppi, and M. A. Sillanpää, Phys. Rev. Applied **11**, 034027 (2019).
[36] R. W. Andrews, T. P. Purdy, K. Cicak, R. W. Simmonds, C. A. Regal, and K. W. Lehnert, Nat. Phys. **11**, 034027 (2019).
[37] D. Malz, and A. Nunnenkamp, Phys. Rev. A **94**, 023803 (2016).
[38] I. Pietikäinen, O. Černotik, and R. Filip, New J. Phys. **22**, 063019 (2020).
[39] H. Xu, A. A. Clerk, and J. G. E. Harris, Nature **568**, 65 (2019).
[40] M. J. Weaver, F. Buters, F. Luna, H. Eerkens, K. Heeck, S. de Man, and J. G. E. Harris, Nat. Commun. **568**, 65 (2019).
[41] U. Kemiktarak, M. Durand, M. Metcalfe and J. Lawall, Phys. Rev. Lett. **113**, 030802 (2014).
[42] A. Oran, S. Ozharar, G. Can, I. Olcer and I. Ozdur, Opt. Express **26**, 376 (2018).
[43] L. Qiu, I. Shomroni, M. A. Ioannou, N. Piro, D. Malz, A. Nunnenkamp, and T. J. Kippenberg, Phys. Rev. A **100**, 053852 (2019).
[44] M. Eichenfield, R. Kamacho, J. Chan, K. J. Vahala, and O. Painter, Nature **459**, 550 (2009).
[45] E. Verhagen, S. Deléglise, S. Weis, A. Schliesser, and T. J. Kippenberg, Nature **482**, 63 (2012).
[46] J. Li, S. Diddams, and K. J. Vahala, Optics Express **22**, 14559 (2014).
[47] B. Hassett, *Introduction into Algebraic Geometry* (Cambridge University Press, Cambridge, 2007).
[48] C. Genes, A. Mari, D. Vitali, and P. Tombesi, Adv. At. Mol. Opt. Phys. **57**, 33 (2009).
[49] M. Karuza, C. Molinelli, M. Galassi, C. Biancofiore, P. Natali, A. Tombesi, G. Di Giuseppe, and D. Vitali, New. J. Phys. **14**, 095015 (2012).
[50] P. E. Kloeden and E. Platen, *Numerical Solution of Stochastic Differential Equations* (Springer-Verlag, Berlin-Heidelberg, 1992).

[51] M. Ludwig, and F. Marquardt, Phys. Rev. Lett. **113**, 073603 (2013).

[52] M. Oudich, S. El-Jallal, Y. Pennec, B. Djafari-Rouhani,J. Gomis-Bresco,D. Navarro-Urrios,C. M. Sotomayor Torres,A. Martínez and A. Makhoute, Phys. Rev. B **89**, 245122 (2014).

[53] L. Mercadé, L. L. Martín, A. Griol, D. Navarro-Urrios and A. Martínez, Nanophotonics **9**, 11 (2020).

[54] D.W. Allan, N. Ashby and C.C. Hodge, *The Science of Timekeeping, Application Note 1289* (Hewlett Packard, 1997).

[55] W. Yu, W. C. Jiang Q. Lin and T. Lu, Nat. Commun. **7**, 12311 (2016).

[56] E. Rubiola *Phase Noise and frequency stability in oscillators* (Cambridge University Press, 2009)
.

[57] X. Luan, Y. Huang Y. Li J. F. McMillan J. Zheng S. Huang P. Hsieh T. Gu D. Wang A. Hati D. A. Howe G. Wen M. Yu G. Lo D. Kwong and C. W. Wong, Sci. Rep. **4**, 6842 (2014)
.

[58] F. Ramian *Time Domain Oscillator Stability Measurement Allan variance* (In: Rhode & Schwarz Application Note 1EF69_E4, 2015)
.

[59] I. Ghorbel, F. Swiadek, R. Zhu, D. Dolfi,G. Lehoucq,A. Martin,G. Moille,L. Morvan,R. Braive,S. Combrié and A. Rossi, APL Photonics **4**, 116103 (2019)
.

[60] S. Tallur, S. Sridaran and S. A. Bhave, Optics Express **19**, 24522-24529 (2011)
.

[61] S. Sridaran and S. A. Bhave, 2012 IEEE 25th International Conference on Micro Electro Mechanical Systems (MEMS) , 664–667 (2012)
.

[62] D. Antonio, D. H. Zanette and D. López, Nat Commun **3**, 806 (2011)
.

[63] U. Kemiktarak, M. Durand, M. Metcalfe and J. Lawall, Phys. Rev. Lett. **13**, 030802 (2014)
.